5-1999

Resonant Tank Motor Model For Voltage Reflection Simulations With PWM Drives

Davia W. Schlegel
Rockwell Automation, dwschlegel@ra.rockwell.com

Glenn T. Wrate
Milwaukee School of Engineering, gwrate@nmu.edu

Russ Kerkman
Rockwell Automation

Gary Skibinski
Rockwell Automation

Resonant Tank Motor Model For Voltage Reflection Simulations With PWM Drives

D. Schlegel* G. Wrate** R. Kerkman* G. Skibinski*

* Rockwell Automation
6400 W. Enterprise Drive
Mequon, WI 53092
(414) 512-7088 (414) 512-8300 Fax

** Milwaukee School of Engineering
1025 N. Broadway
Milwaukee, WI 53202

Abstract: Reflected wave transient voltages that are impressed on drive output cables and low voltage ac induction motors are normally simulated with steep fronted *dv/dt* pulse waveforms from PWM voltage source inverters. System simulation arises from a need to correlate reflected wave peak voltage and risetime with the dielectric insulation capability of both the motor and cable. To obtain reasonable results, accurate models of each component must be employed. This investigation will concentrate on parameter identification for a high frequency resonant tank motor model from fractional to several hundred horsepower.

I. Introduction

The increasing use and issues associated with PWM drives has caused applications engineers to approach installations with caution. The use of accurate component models provides the designer with a measure of comfort in the systems performance. Numerous simulation packages have become available over the years, such as Transient Network Analyzer's (TNA's) in the 1930's, Electro Magnetic Transients Program (EMTP) in the late 1970's [1], PSpice in 1984 [2] and MATLAB in 1990 [3]. PSpice is among the more popular simulation tools, due to its availability and numerous developed models. MATLAB has spawned SIMULINK, the object-oriented language used in this paper.

II. Drive System Model

Ac drive systems have become increasingly complex and require simulations to aid their design. The complexity of a simulation is dictated by the particular subsystem analyzed. Evaluation of high frequency effects necessitates simulation times based on the smallest eigenvalues. The desired accuracy places constraints on the simulation package and corresponding component models. Recently, a SIMULINK based drive system tool was proposed [4]. The simulation separated the application into three subsystems, drive (source), cable (transport delay), and machine (load). The transport delay feature of the program was used to simulate the traveling wave propagation time fairy accurately. Cable skin and proximity effects of cable resistance may be modeled easily. The source – using a step function - models the IGBT risetime from the drive. The motor was modeled with a combination of motor surge impedance, stator resistance, high frequency capacitance and winding inductance. Many of the parameters of the system are not readily known through published literature or are difficult to predict. Therefore, this investigation will concentrate on motor model parameter identification from fractional to several hundred horsepower.

III. Motor Model

The adverse effects of steep voltage wavefronts on machine windings have resulted in extensive investigations into motor terminal overvoltages [5-10]. IGBT based PWM voltage source inverters, with very small rise times, subject ac induction motors to extreme voltage stress thousands of times per second. Peak line-to-line terminal over-voltage (*Vpk*) at the receiving end of an *initially uncharged* transmission line subjected to a *single PWM pulse* with risetime (*tr*), is derived in [11].

A. High Frequency Models of AC Motors

Numerous investigations into high frequency modeling of ac induction machines were recently reported [12-17]. High frequency motor models may be subdivided into two broad categories: Finite Element Analysis (FEA) and reduced order models. FEA models examine the machine on a per turn level [12], but they are complex and primarily for motor design purposes. Reduced order models are developed for simulation tools designed to examine application specific problems [4,9,14].

B. Motor Model for Differential Reflected Wave Simulations

As derived in [4,10], a differential or line-to-line motor model for purposes of predicting the peak line-to-line motor terminal voltage (*Vt*) is set forth in Fig. 1. The circuit topology, essentially a resonant tank, provides a relatively simple interface to transmission line models.

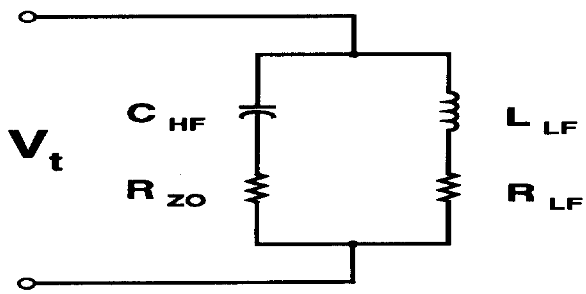

Fig. 1. Differential Mode Motor Model.

0-7803-5293-9/99 $10.00 © 1999 IEEE

The parameters are obtainable through system identification procedures and tabulated motor data. At low frequency, the motor behaves as an inductive dominant series impedance (R + jωL). At high frequency, the motor behaves as a capacitive dominant series impedance (R + 1/jωC). In Fig. 1, the low frequency inductance, L_{LF}, (consistent with low frequency motor analysis) is in series with the low frequency stator resistance, R_{LF}. The high frequency resistance, R_{Z0}, corresponds to the surge impedance of the machine and establishes the reflection coefficient, with the high frequency capacitance, C_{HF}, appearing as a short.

C. LCR Measurements and Trends in Motor Impedance and Phase Angle.

A Hewlett Packard Impedance Analyzer (HP4284), with a frequency range of 20 Hz to 1 MHz, was used to measure the impedance and phase angle of over 30 motors across a broad range of horsepower. The impedance magnitude and phase angle changed with excitation frequency. At low frequency, all the machines had an inductive dominant series impedance (R + jωL), which turned into a capacitive dominant series impedance (R + 1/jωC) after a resonant maximum is exceeded. The phase angle switched from inductive (positive) to capacitive (negative) at the resonant maximum point. Higher frequency measurements were recorded to demonstrate additional oscillations, but exceeded device limits. The Impedance vs. Frequency plots for 1, 10, and 100 hp machines from various vendors are shown in Fig. 2. A range of motor horsepower impedance from a single vendor is shown in Fig. 3.

To verify the symmetry of the windings, the three motor phases were sequentially transposed and measured in each grouping. Identical motors were also measured. When plotted, both cases showed good agreement. Impedance variations occurred within identical horsepower rated machines with different frame sizes. Fig. 4 indicates the stator dimensions and frame material affect the impedance. Fig. 5 shows impedance variations within a single NEMA frame size from different vendors, indicating the manufacturing process effects.

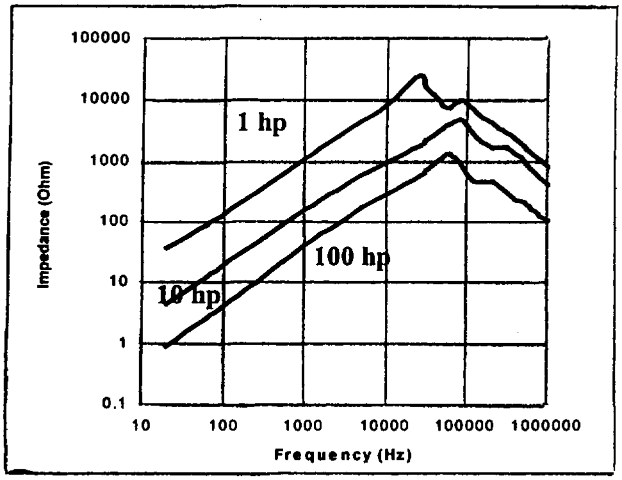

Fig. 2. Impedance Magnitude for 1, 10, and 100 hp Motors.

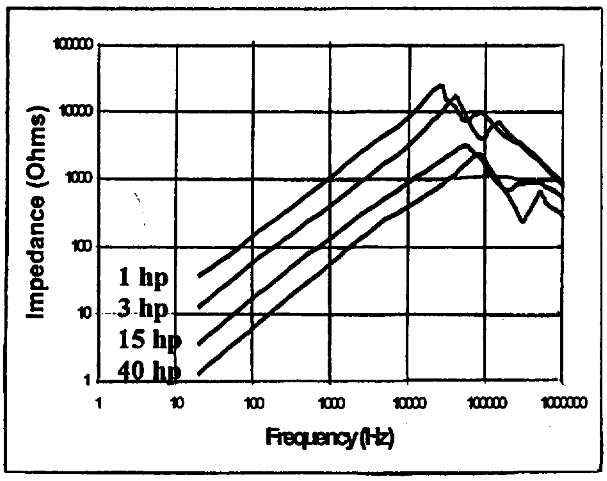

Fig. 3. Impedance Magnitude for 1, 3, 15, and 40 hp Motors from the Same Manufacturer.

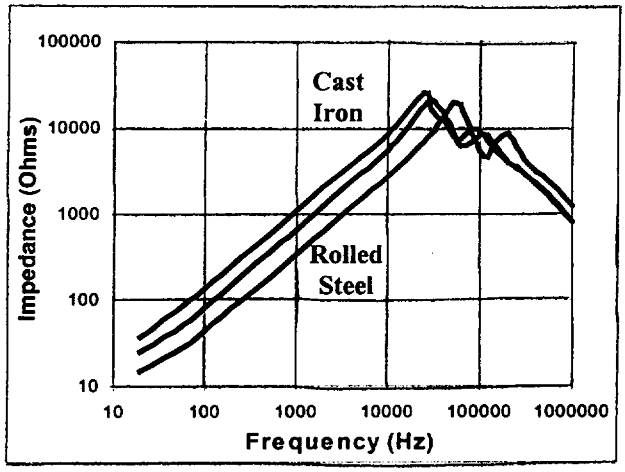

Fig. 4. Impedance Magnitude for Three 1 hp Motors with Different Frame Styles.

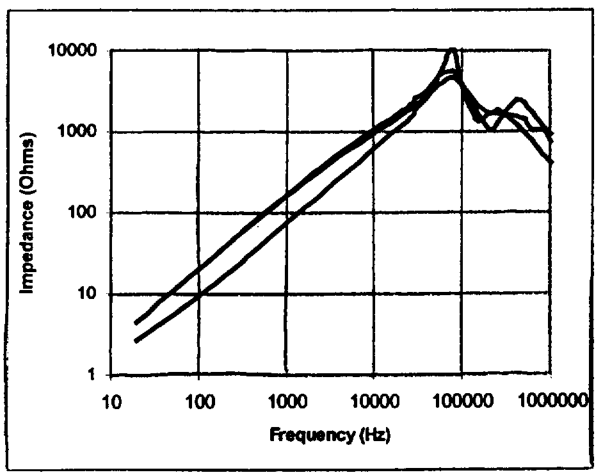

Fig. 5. Impedance Magnitude for Three 10 hp Motors From Different Vendors in the Same Frame.

Several trends are apparent from the data in Figs. 2-5. First, the low frequency portion (inductive branch) has a similar slope across the range of motor impedance. Second, as motor horsepower increases, the low frequency impedance value decreases. These provide hints about the R_{LF} and L_{LF} values. Third, the resonant maximum point migrates higher with increasing horsepower. Fourth, the high frequency portion (capacitive branch) has a dominant minor oscillation after the maximum point. These provide hints about the R_{Z0} and C_{HF} values. Ongoing work will develop equations to model R_{LF}, L_{LF}, C_{HF}, and R_{Z0} as a function of horsepower.

D. Identifying Motor Surge Impedance (R_{Z0})

Identifying R_{Z0} using Inverter Pulses: The apparent R_{Z0} observed during the rising edge of the reflected wave front was measured under drive operation [4]. Fig. 9 of [4] shows how R_{Z0} varies with horsepower when measured during the pulse risetime. Motor surge impedance is not an absolute value, since 1 hp measured values varied from 1,000 to 5,000 ohms depending on the manufacturer. Thus, rather than an absolute R_{Z0} magnitude vs. horsepower line, there is probably a band for model use.

Identifying R_{Z0} with LCR Analyzer: HP4284 test leads were connected from parallel motor phases A & B to phase C to simulate the surge impedance observed during a reflected wave transient. Motor surge impedance is inferred from the high frequency capacitive dominant impedance. When the LCR readings are capacitive, the corresponding resistance is the surge impedance.

E. Identifying High Frequency Capacitance (C_{HF})

The high frequency capacitance, C_{HF}, can be inferred from the high frequency capacitive dominant impedance that occurs after the resonant maximum point. The capacitance is hard to quantify, due to the multitude of winding configurations possible [14].

F. Identifying Low Frequency Inductance (L_{LF})

The low frequency inductance, L_{LF}, is consistent with traditional motor loads used in low frequency simulations, where a series RL load is used. The L_{LF} can be inferred from the low frequency inductive dominant impedance.

G. Identifying Low Frequency Resistance (R_{LF})

The low frequency resistance, R_{LF}, is consistent with traditional motor loads used in low frequency simulations, where a series RL load is used. The R_{LF} can be inferred from the low frequency inductive dominant impedance.

VI. Conclusion

A high frequency resonant tank circuit motor model was developed for use in simulations of drive systems. LCR Impedance Analyzer measurements were recorded to verify the low frequency inductive impedance ($R + j\omega L$), a resonant maximum, and the high frequency capacitive impedance ($R + 1/j\omega C$). The low frequency impedance was developed into a series resistance (R_{LF}) and inductance (L_{LF}), while the high frequency was developed into a series surge impedance (R_{Z0}) and capacitance (C_{HF}). The LCR impedance data was correlated and trends were established to assist in model parameter identification. Ongoing work will develop empirically derived equations for R_{LF}, L_{LF}, C_{HF}, and R_{Z0} as a function of horsepower.

References

[1] H. Dommel, *Electro-magnetics Transients Program & Theory Manual*, Bonneville Power Administration, Portland, OR

[2] MicroSim Pspice, MicroSim Corporation.

[3] SIMULINK with Matlab, The Mathworks, Inc.

[4] G. Skibinski, R. Kerkman, D. Leggate, J. Pankau, and D. Schlegel, "Reflected Wave Modeling Techniques for PWM AC Motor Drives", IEEE APEC Conference, Anaheim, CA, Feb 15-19 1998, pp. 1021 - 1029.

[5] P. Van Paucke, R. Belmans, W. Geysen, and E. Ternier, "Overvoltages in Inverter Fed Induction Machines Using High Frequency Power Electronic Components," IEEE APEC Conference Proceeding 1994, pp. 536-541.

[6] T. Takahashi, M. Termeyer, T. Lowery, and H. Tsai, "Motor Lead Length Issues for IGBT drives", IEEE Pulp and Paper Conference Proceedings, 1995, pp. 21-27.

[7] C. J. Melhorn and L. Tang, "Transient Effects of PWM ASDs on Standard Squirrel Cage Induction Motors," IEEE IAS Conference, Orlando, FL, Oct. 8-12, 1995, pp. 2689-2695.

[8] B. Kawkabani, J.J. Simond, and F. Kehtari, "Voltage Peaks of Low Voltage Motors Due to PWM Inverter Supply," EPE Conference Proceedings 1995, Sevilla, pp. 465-469.

[9] A. von Jouanne, P. Enjeti, and W. Gray, "The Effect of Long Motor Leads on PWM Inverter Fed AC Motor Drive Systems," IEEE APEC Conference, Dallas, TX, March 6-9, 1995, pp. 592-597.

[10] R. Kerkman, D. Leggate, G. Skibinski, "Interaction of Drive Modulation & Cable Parameters on AC Motor Transients," IEEE IAS Conference, San Diego, CA, Oct. 6-10, 1996, pp. 143-152.

[11] G. Skibinski, "Design Methodology of a Cable Terminator to Reduce Reflected Voltage on AC Motors", IEEE IAS Conference, San Diego, CA, October 6-10, 1996, pp. 153-161.

[12] G. Suresh, Hamid A. Toliyat, Dudi A. Rendussara, and Prasad N. Enjeti, "Predicting the Transient Effects of PWM Voltage Waveform on the Stator Windings of Random Wound Induction Motors," IEEE APEC Conference, Atlanta, GA, Feb 23-27, 1997, pp. 135-141.

[13] G. Grandi, D. Casadei, A. Massarini, "High Frequency Lumped Parameter Model for AC Motor Windings", EPE Conference, Trondheim, September 1997, pp. 2.578-2.583.

[14] G. Grandi, D. Casadei, U. Reggiani, "Analysis of Common Mode and Differential Mode HF Current Components in PWM Inverter FED AC Motors," IEEE PESC'98 Conference, Fukuoka, Japan, May 17-22, 1998, pp. 1146-1151.

[15] A Consoli, G. Oriti, A. Testa, and A. L. Julian, "Induction Motor Modeling for Common Mode and Differential Mode Emission Evaluation," IEEE IAS Conference, San Diego, CA, Oct. 6-10 1996, pp. 595-599.

[16] David B. Hyypio, " Effects of Risetime and Cable Length on Motor Insulation Degradation Resulting from Operation on PWM Voltage Source Inverters," IEEE International Electric Machines and Drives Conference, IEMDC Record, May 1997, pp. TCS-2.1-TCS-2.3.

[17] D. Hyypio, "Simulation of Cable and Winding response to Steep Fronted Voltage Waves", IEEE IAS Conference, Orlando, FL, Oct. 8-12, 1995, pp. 800-806.